

Introduction: We propose the use of a recent bi-dimensional fuzzy entropy to process colored images ($FuzEn_{C2D}$). This algorithm processes color channels independently, with both global and local characteristics consideration. FuzEn2D was tested regarding sensitivity to parameters (tolerance and embedding dimension), rotation, irregularity discrimination, and its consistency. For these validation tests, white noise (WGN) and colored Brodatz textures were used. In addition, $FuzEn_{C2D}$ was tested on the PH2 dataset [1] using common nevi, atypical nevi, and melanoma lesions dermoscopic images.

Results: The $FuzEn_{C2D}$ shows low-sensitivity to tolerance values (see Fig.3). Besides, it also shows to be a consistent metric regarding the different tested sizes (Fig.4). Moreover, as expected, the entropy increases when the images are shuffled, increasing, therefore, their entropy (Table 1). In Table 2, it can be verified that the $FuzEn_{C2D}$ does not change significantly upon image rotation. In Table 3, we can verify that for at least one color channel is possible to differentiate two different lesions.

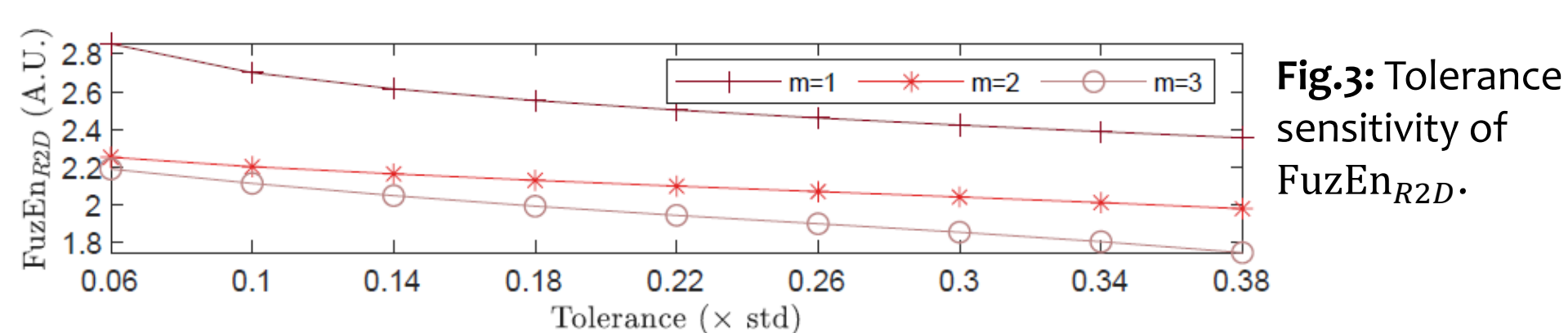


Fig.3: Tolerance sensitivity of $FuzEn_{R2D}$.

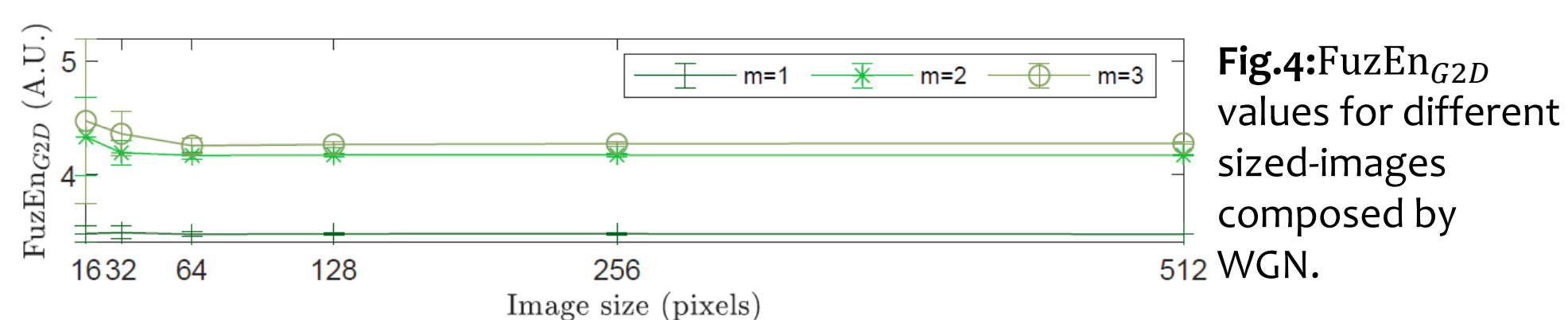


Fig.4: $FuzEn_{G2D}$ values for different sized-images composed by WGN.

Img #	$FuzEn_{R2D}$		$FuzEn_{C2D}$		$FuzEn_{B2D}$	
	Original	Shuffled	Original	Shuffled	Original	Shuffled
1	6.401 ± 0.106	12.049 ± 0.525	6.899 ± 0.124	12.633 ± 0.617	5.818 ± 0.193	11.319 ± 0.241
2	3.678 ± 0.293	10.889 ± 0.469	4.239 ± 0.371	12.693 ± 0.716	3.152 ± 0.287	10.095 ± 0.350
3	2.018 ± 0.353	7.404 ± 1.011	2.007 ± 0.346	7.539 ± 0.908	2.059 ± 0.349	7.530 ± 1.100
4	0.595 ± 0.029	4.238 ± 0.250	0.695 ± 0.057	4.600 ± 0.288	0.569 ± 0.031	4.308 ± 0.244
5	1.034 ± 0.183	8.296 ± 0.801	1.340 ± 0.218	9.662 ± 0.894	1.175 ± 0.190	8.813 ± 0.808
6	0.720 ± 0.034	7.131 ± 0.890	0.854 ± 0.053	5.550 ± 0.206	1.482 ± 0.327	12.575 ± 1.828

Table 1: $FuzEn_{2GD}$ values for original Brodatz textures and their shuffled versions.

Img #	Orig.	$FuzEn_{R2D}$			$FuzEn_{C2D}$		
		90°	180°	Orig.	90°	180°	
1	6.401 ± 0.106	6.401 ± 0.106	6.403 ± 0.106	6.899 ± 0.124	6.899 ± 0.124	6.901 ± 0.124	
2	3.678 ± 0.293	3.679 ± 0.293	3.678 ± 0.292	4.239 ± 0.371	4.240 ± 0.371	4.238 ± 0.370	
3	2.018 ± 0.353	2.017 ± 0.354	2.019 ± 0.355	2.007 ± 0.346	2.006 ± 0.348	2.008 ± 0.349	
4	0.595 ± 0.029	0.595 ± 0.028	0.595 ± 0.029	0.695 ± 0.057	0.694 ± 0.056	0.694 ± 0.056	
5	1.034 ± 0.183	1.031 ± 0.180	1.030 ± 0.179	1.340 ± 0.218	1.336 ± 0.212	1.336 ± 0.213	
6	0.720 ± 0.034	0.719 ± 0.034	0.719 ± 0.034	0.854 ± 0.053	0.854 ± 0.053	0.855 ± 0.053	

	$FuzEn_{B2D}$		
	Orig.	90°	180°
	5.818 ± 0.193	5.818 ± 0.193	5.820 ± 0.193
	3.152 ± 0.287	3.152 ± 0.287	3.151 ± 0.287
	2.059 ± 0.349	2.057 ± 0.351	2.059 ± 0.351
	0.569 ± 0.031	0.568 ± 0.029	0.568 ± 0.030
	1.175 ± 0.190	1.171 ± 0.185	1.171 ± 0.185
	1.482 ± 0.327	1.481 ± 0.330	1.483 ± 0.328

Table 2: $FuzEn_{2GD}$ values for original Brodatz textures and their rotated versions.

$FuzEn_{C2D}$	p -value
CNG vs. ANG	0.004
$FuzEn_{R2D}$	
CNG vs. MG	0.000
ANG vs. MG	0.054
$FuzEn_{G2D}$	
CNG vs. ANG	0.136
CNG vs. MG	0.000
ANG vs. MG	0.034
$FuzEn_{B2D}$	
CNG vs. ANG	0.637
CNG vs. MG	0.009
ANG vs. MG	0.068

Table 3: p -values for $FuzEn_{2GD}$ values of melanoma group (MG), common nevi group (CNG), and atypical nevi group (ANG). The * represents statistical significance for $p < 0,05$.

Methods:

- FuzEn2D concept:** Consider an image $U(i, j, k)$ of $W \times L$ (W -width, L -length) pixels with $1 \leq i \leq W$, $1 \leq j \leq L$, and k channels. In this case, $k=R, G, \text{ and } B$ (Red, Green, and Blue). A squared template of embedding dimension and k channel is defined as:

$$\mathbf{X}_{ijk}^m = \begin{bmatrix} U_{i,j,k} & \cdots & U_{i,j+m-1,k} \\ \vdots & \ddots & \vdots \\ U_{i+m-1,j,k} & \cdots & U_{i+m-1,j+m-1,k} \end{bmatrix}$$

From this point forward \mathbf{X}_{ijk}^m is represented as $t_{\alpha,k}^m$, where $\alpha = i, j$. The number of possible comparisons is $N_m = (W - m)(L - m)$. The distance between two templates is $d_{\alpha,\beta}^k = \max |t_{\alpha,k}^m - t_{\beta,k}^m|$. The similarity degree is defined as $D_{\alpha,\beta,k} = \exp\left(-\left(\frac{d_{\alpha,\beta}^k}{r}\right)^n\right)$.

The similarity average is $\Phi^m = \frac{1}{N_m^2} = \sum_{\alpha} \sum_{\beta} D_{\alpha,\beta,k}$. These steps are repeated for $m+1$ squared templates for the k channels, to obtain the entropy value of each of channel as $FuzEn_{C2D} = \ln\left(\frac{\Phi^m}{\Phi^{m+1}}\right)$.

- Sensitivity to tolerance (r):** use of an image taken from Brodatz texture of 256×256 pixels (Fig. 1c).
- Sensitivity to embedding dimension (m) and consistency:** use of squared WGN based colored images with an edge size of 32, 64, 128, 256, and 512 pixels, and $n = 2$, $m = 1, 2, 3$, and $r = 0, 2 \times SD_{data}^k$ (see Fig.2).
- Sensitivity to rotation and shuffling tests:** use of 10 sub-images of 256×256 pixels of Brodatz textures (examples on Fig.1) obtained randomly ($n = 2$, $m = 2$, and $r = 0, 2 \times SD_{data}^k$).
- Evaluation of colored dermoscopic images:** Analysis of Common nevi, atypical nevi, and melanoma Ph2 dataset images using $FuzEn_{C2D}$ values with $n = 2$, $m = 2$, and $r = 0, 2 \times SD_{data}^k$. To verify the existence of significant statistical differences ($p < 0,05$), the Kruskal-Wallis test was used.

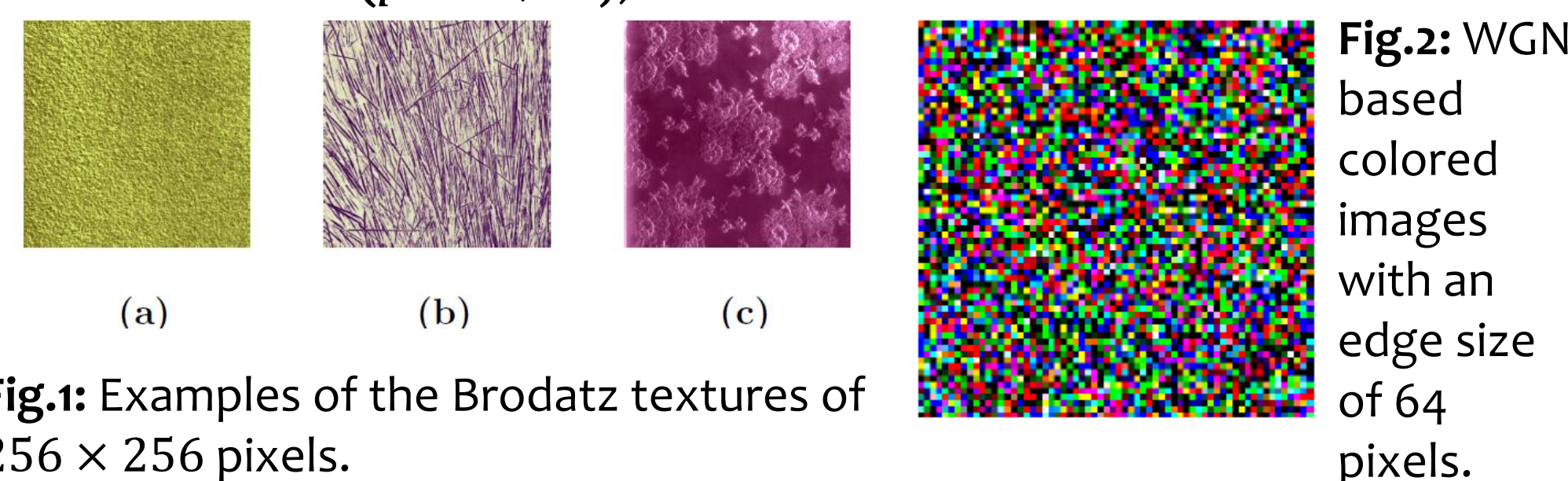


Fig.1: Examples of the Brodatz textures of 256×256 pixels.

Conclusion: For a future analysis, it would be interesting to use these $FuzEn_{C2D}$ values as texture-based feature to an early diagnosis and identification of melanoma. Moreover, this algorithm shows a relatively low sensitivity to parameters. Even when images are rotated, the algorithm is relatively insensitive. In addition, this colored metric is able to discriminate irregularity, as expected.

Reference: [1] Teresa Mendonça, Pedro M. Ferreira, Jorge S. Marques, André R. S. Marçal, and Jorge Rozeira. "PH2 - A dermoscopic image database for research and benchmarking". In: 2013 35th Annual International Conference of the IEEE Engineering in Medicine and Biology Society (EMBC). IEEE, 2013. doi: 10.1109/embc.2013.6610779

Acknowledgment: This work was supported by FCT (Fundação para a Ciência e Tecnologia) under the project UID/04559/2020 to fund the activities of Laboratory for Instrumentation, Biomedical Engineering and Radiation Physics), and by the European Regional Development Fund, Competitiveness and Internationalization Operational Programme (PT-COMPETE 2020) under the project PTDC/EMD-TLM/30295/2017.